Research article

AGBL2 promotes renal cell carcinoma cells proliferation and migration via α-tubulin detyrosination

Wei Liu [a,b], Yifei Zhang [a,b], Yechen Nie [b], Yifu Liu [b], Zhongqi Li [b], Zhicheng Zhang [b], Binbin Gong [b,**], Ming Ma [a,b,c,*]

[a] Department of Urology, Gaoxin Branch of The First Affiliated Hospital of Nanchang University, Nanchang, 330000, China
[b] Jiangxi Provincial Key Laboratory of Urinary System Diseases, Department of Urology, The First Affiliated Hospital, Jiangxi Medical College, Nanchang University, Nanchang, Jiangxi, China
[c] Department of Urology, Gaoxin Branch of The First Affiliated Hospital, Jiangxi Medical College, Nanchang University, Nanchang, 330000, China

ABSTRACT

Background: AGBL2's role in tumorigenesis and cancer progression has been reported in several cancer studies, and it is closely associated with α-tubulin detyrosination. The roles of AGBL2 and α-tubulin detyrosination in renal cell carcinoma (RCC) pathogenesis remain unclear and require further investigation.
Methods: In this study, we conducted an analysis of AGBL2 expression differences between renal clear cell carcinoma tissues and normal tissues using data from The Cancer Genome Atlas (TCGA). We performed a comprehensive prognostic analysis of AGBL2 in Kidney Renal Clear Cell Carcinoma (KIRC) using univariate and multivariate Cox regression. Based on the results of the Cox analysis, we constructed a prognostic model to assess its predictive capabilities. Receiver Operating Characteristic (ROC) analysis confirmed the diagnostic value of AGBL2 in renal cancer. We conducted further validation by analyzing cancer tissue samples and renal cancer cell lines, which confirmed the role of AGBL2 in promoting RCC cell proliferation and migration through in vitro experiments. Additionally, we verified the impact of AGBL2's detyrosination on α-tubulin using the tubulin carboxypeptidase (TCP) inhibitor parthenolide. Finally, we performed sequencing analysis on AGBL2 knockdown 786-O cells to investigate the correlation between AGBL2, immune infiltration, and AKT phosphorylation. Moreover, we experimentally demonstrated the enhancing effect of AGBL2 on AKT phosphorylation.
Results: TCGA analysis revealed a significant increase in AGBL2 expression in RCC patients, which was correlated with poorer overall survival (OS), disease-specific survival (DSS), and progression-free intervals (PFI). According to the analysis results, we constructed column-line plots to predict the 1-, 3-, and 5-year survival outcomes in RCC patients. Additionally, the calibration plots assessing the model's performance exhibited favorable agreement with the predicted outcomes. And the ROC curves showed that AGBL2 showed good diagnostic performance in KIRC (AUC = 0.836)). Cell phenotyping assays revealed that AGBL2 knockdown in RCC cells significantly inhibited cell proliferation and migration. Conversely, overexpression of AGBL2 resulted in increased cell proliferation and migration in RCC cells. We observed that AGBL2 is predominantly located in the nucleus and can elevate the detyrosination level of α-tubulin in RCC cells.

Moreover, the enhancement of RCC cell proliferation and migration by AGBL2 was partially inhibited after treatment with the TCP inhibitor parthenolide. Analysis of the sequencing data revealed that AGBL2 is associated with a diverse array of biological processes, encompassing signal transduction and immune infiltration. Interestingly, AGBL2 expression exhibited a negative correlation with the majority of immune cell infiltrations. Additionally, AGBL2 was found to enhance the phosphorylation of AKT in RCC cells.

Conclusion: Our study suggests that AGBL2 fosters RCC cell proliferation and migration by enhancing α-tubulin detyrosination. Moreover, elevated AGBL2 expression increases phosphorylation of AKT in RCC cells.

1. Introduction

Renal cell carcinoma (RCC) stands among the top 10 most prevalent cancers, representing 90 % of kidney tumors [1]. The incidence of RCC has shown a rise, contributing to the socio-medical and economic burden [2]. The primary histological subtypes comprise Kidney renal clear cell carcinoma (KIRC), Kidney renal papillary cell carcinoma (KIRP)and other less common variants. Conventional radiotherapy and chemotherapy prove ineffective in managing metastatic RCC patients. Despite advancements in our comprehension of RCC and the emergence of targeted therapy and immunotherapy, the 5-year survival rate for metastatic RCC patients hovers around 12 % [3]. Challenges persist in investigating individuals with locally advanced and distant metastatic kidney cancer. Therefore, the pursuit of innovative diagnostic and therapeutic targets in kidney cancer is of critical importance.

Microtubules (MTs), composed of α- and β-tubulin subunits, are vital components of the cell's cytoskeleton and are integral to organelle construction. They are actively engaged in essential biological functions, such as cell growth and motility [4,5]. Exhibiting dynamic instability, these subunits undergo continuous transformations throughout the cell cycle [5]. The diversity and stability of MTs' functions are achieved through microtubule-associated proteins (MAPs) and the post-translational modifications of tubulin. These modifications encompass polyglutamylation, polyglycylation, phosphorylation, acetylation, tyrosination, and detyrosination, with a significant role in cancer signaling regulation [6]. These post-translational modifications play a crucial role in regulating various cellular processes and contribute to the intricate functionality of microtubules within the cell. Predominantly occurring at the C-terminus of tubulin [7], these modifications have been particularly noted for their relevance to MT stability, as recent research has revealed that detyrosination of α-tubulin's C-terminal Tyr residue fortifies MT stability [8]. The detyrosination of α-tubulin serves as a crucial regulatory signal for mitosis and muscle mechanotransduction [9]. Abnormal levels of α-tubulin detyrosination have been correlated with various pathological states, such as increased tumor aggressiveness [10], the onset of neuronal disorders [11], heart failure [12], and cardiomyopathy [13]. This post-translational modification, mediated by microtubule carboxypeptidase, is also intricately connected to cancer drug resistance and progression [14–16]. Lopes et al. [14] reported that α-tubulin detyrosination increased the cytotoxicity of paclitaxel in paclitaxel-sensitive cancer cells, however unfortunately this effect was ineffective in paclitaxel-resistant cells. Some studies have reported that the tubulin tyrosine ligase during tumour cell invasion increases the α-tubulin detyrosination and thus promotes microtentacle production, thereby enhancing the reattachment of circulating tumour cells to the vascular endothelium during metastasis [15]. This may indicate that the α-tubulin detyrosination is closely related to tumour cell migration. Iida-Norita et al. [16] reported that VASH2, a molecule with tubulin carboxypeptidase activity, increases microtubule protein detyrosination and promotes metastasis of pancreatic ductal adenocarcinoma. The exact mechanism of α-tubulin detyrosination in cancer cells and its regulatory targets are still unclear, however, studies have indicated that the regulation of α-tubulin detyrosination may indirectly affect the migration and death of cancer cells, which is worthy of further investigation.

AGBL Carboxypeptidase 2 (AGBL2), also known as Cytoplasmic Carboxypeptidase 2 (CCP2), has been recently identified as a microtubule carboxypeptidase. Emerging evidence has revealed that AGBL2 plays a contributory role in the development of various tumors, including those of the liver, breast, and kidney [17–19]. It has been associated with the promotion of tumorigenesis and correlated with unfavorable prognosis in patients. However, the specific role and underlying mechanisms of AGBL2 in RCC pathogenesis continue to be unclear and warrant further investigation.

In this study, we delineated the role of AGBL2 in augmenting α-tubulin detyrosination, thereby facilitating RCC cell proliferation and metastasis, and further uncovered its capacity to enhance AKT phosphorylation. Additionally, our investigations have extended to uncover its influence on various signaling pathways and immune infiltration within RCC cells. Collectively, these findings underscore AGBL2 as a promising novel prognostic marker, and they highlight its potential as a therapeutic target for human RCC.

2. Materials and methods

2.1. Tissue specimens and cell lines

Cancerous and adjacent normal tissues from renal cancer patients were procured from the First Affiliated Hospital of Nanchang University, following the acquisition of informed consent and with the endorsement of the Ethics Committee. Renal cancer cell lines (786-O and OSRC-2) and human renal tubular epithelial cells (HEK293T) were purchased from Procell Life Science&Technology (Wuhan, China). All cells were subjected to STR authentication in Procell Life Science&Technology. The aforementioned cell lines were cultivated in RPMI 1640 (786-O and OSRC-2) and DMEM(HEK293T) media. These media were enriched with penicillin,

streptomycin, and 10 % fetal bovine serum (FBS). The cells were maintained at 37 °C within a humidified incubator environment containing 5 % CO2.

2.2. Real-time quantitative PCR and sequencing

Total RNA was extracted utilizing TRIzol reagent, followed by the synthesis of complementary DNA (cDNA) via reverse transcription employing the EasyScript cDNA Synthesis SuperMix (Transgen Biotech, China). Real-time quantitative PCR (qPCR) assays were executed using TransStart Top Green qPCR SuperMix (+Dye II) (Transgen Biotech, China). The housekeeping gene β-Actin was utilized as the internal control for normalization, and the relative quantity of RNA was determined employing the comparative Ct method ($2^{\wedge}(-\Delta\Delta CT)$). Primer sequences pertinent to this study are delineated in Supplementary File 1. Furthermore, RNA libraries were meticulously sequenced on the Illumina Novaseq™ 6000 platform, facilitated by OE Biotech, Inc., Shanghai, China.

2.3. Western Blotting

Whole-cell lysates were methodically prepared, incorporating protease and phosphatase inhibitor cocktails to preserve protein integrity. Subsequent determination of protein concentrations was conducted utilizing the Bicinchoninic Acid (BCA) protein assay. Equivocal quantities of protein were resolved on 10 % SDS-polyacrylamide gel electrophoresis (PAGE) and duly transferred to Polyvinylidene Difluoride (PVDF) membranes. Thereafter, the membranes were blocked with 5 % non-fat milk at ambient temperature and incubated overnight with specific primary antibodies (details provided in Supplementary File 1) at 4 °C. Visualization of the protein blotting results was facilitated by an enhanced chemiluminescence (ECL) detection system, with subsequent quantification accomplished using ImageJ software (version 1.52). For quantitative analysis of Western Blotting results, grayscale values of Western Blotting bands were measured using Image J and statistically analyzed using GraphPad Prism 8 by selecting the appropriate method and plotting the pictures. Each experiment was repeated at least 3 times.

2.4. Immunohistochemistry (IHC)

We used tumour and peritumour tissue specimens from six patients with kidney cancer for follow-up experiments. Tissue samples underwent a series of preparative steps including fixation in 10 % formalin, dehydration through graded ethanol, embedding in paraffin, and sectioning for microscopic analysis. The thickness of the slices was standardised at 4 μm and adjusted appropriately according to the results of subsequent experiments. The range was bounded by 2–6 μm. Following the dewaxing and rehydration stages, antigen retrieval was facilitated by heating the slides in sodium citrate buffer. The sections were then blocked with 1 % Bovine Serum Albumin (BSA) and incubated with anti-AGBL2 primary antibodies at 4 °C overnight. Subsequent treatment involved exposure to a secondary antibody at 37 °C for 1 h, chromogenic visualization with diaminobenzidine, and counterstaining with hematoxylin to enhance contrast. The resultant images were acquired utilizing a Zeiss microscope and subsequently subjected to analysis through ImageJ software (version 1.52). The percentage of area occupied by positive staining of sections at 40× was analyzed using ImageJ. The appropriate statistics were selected for statistical analysis and plotted using GraphPad Prism 8. Each experiment was repeated at least 3 times.

2.5. Immunofluorescence

Cells were methodically seeded onto coverslips and permitted to adhere over a 24-h period. Subsequent fixation was achieved using 4 % paraformaldehyde for a duration of 30 min at ambient temperature. Following fixation, the cells were subjected to an immunofluorescence protocol using a specialized reagent kit (Elabscience Biotechnology, Wuhan, China) and were then meticulously mounted onto microscope slides. Visualization and image capture were conducted with a confocal laser microscope system (Stellaris 5, Leica), and the resulting images were finely adjusted and analyzed using the FV10-ASW4.2 viewer software.

2.6. Cell transfection

SiRNA was synthesized by RiboBio (Guangzhou, China) and subsequently transfected into target cells employing Lipofectamine 2000 (Invitrogen), strictly adhering to the manufacturer's prescribed protocol. For the generation of virus particles, HEK293T cells were infected with pLenti-CMV-AGBL2-GFP-Puro in conjunction with two packaging plasmids (psPAX2 and pMD2.G); Both an empty vector and Si-NC were judiciously employed as controls to ensure the integrity and validity of the experimental conditions under investigation. The harvested virus particles were then utilized to infect 786-O and OSRC-2 cell lines with the aim of establishing AGBL2-overexpressing derivatives. Selection of stably transfected cells was executed through the application of 2 mg/ml puromycin for a time frame of 48 h.

2.7. Cell phenotyping assay

Cells were meticulously harvested through trypsin digestion to yield a uniform single-cell suspension, subsequently quantified using an electronic cell counter (BioRad). The Transwell migration assay was executed in the following manner: $4 \times 10^{\wedge}4$ treated cells were resuspended in 200 μl of serum-free medium and precisely seeded into the upper chamber of Transwell plates, while the lower
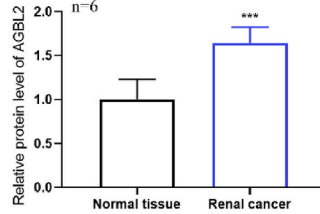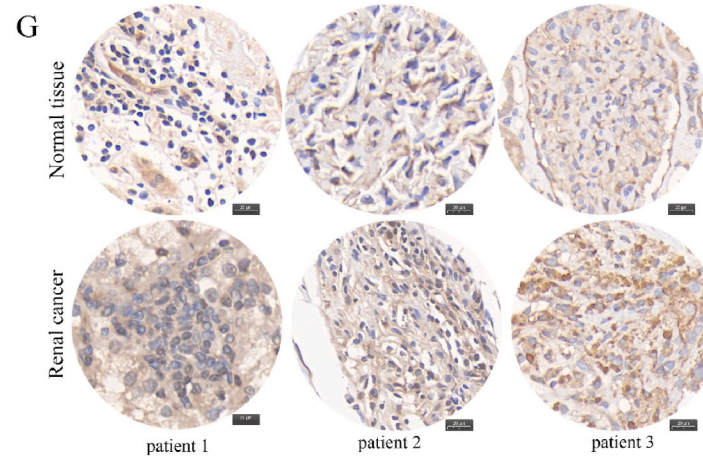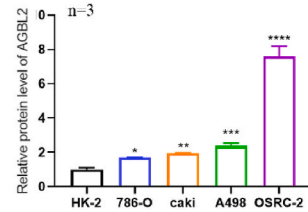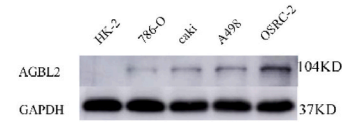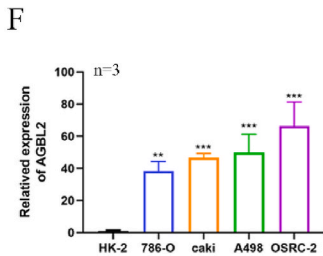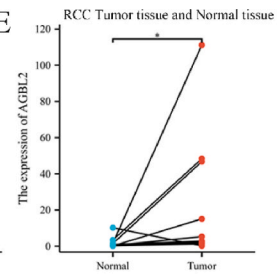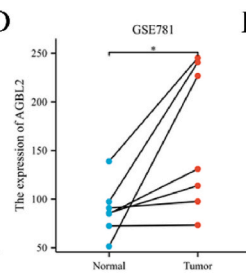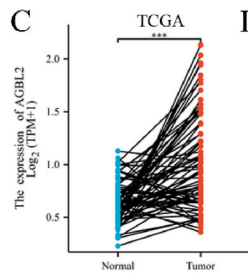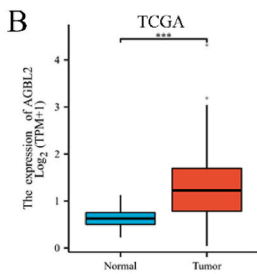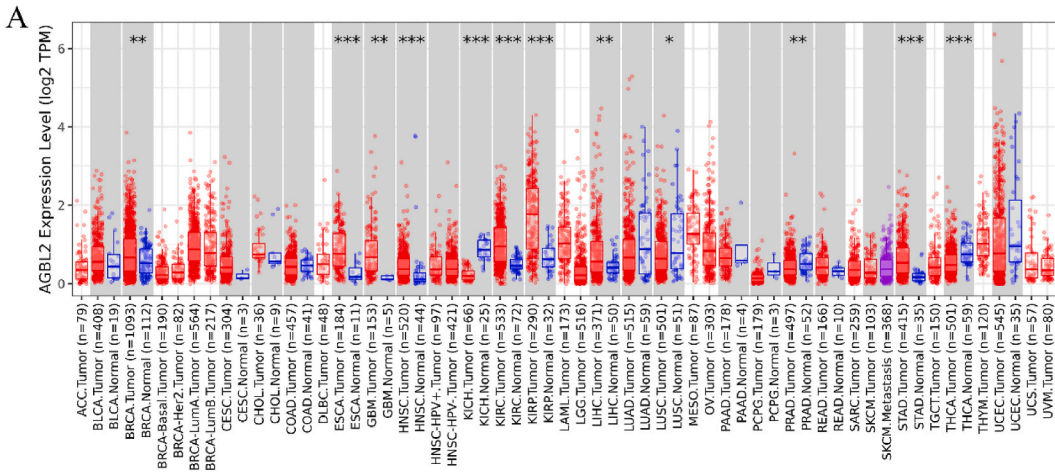
(caption on next page)

Fig. 1. AGBL2 is upregulated in renal cell carcinoma (A) A pan-cancer analysis of AGBL2 expression utilizing TIMER 2.0. (B, C) Analysis of AGBL2 expression in both unpaired and paired renal cancer tissues from the TCGA database. (D) Examination of AGBL2 expression levels within the GEO dataset GSE781. (E, F) Validation of AGBL2 expression across renal cancer tissues and cell lines. The results of Western Blotting demonstrate the protein levels of AGBL2 in the cell line, which were quantified using histograms. Data (n = 3)were analyzed, with statistical significance denoted as *p < 0.05; **p < 0.01; ***p < 0.001; ****p < 0.0001. (G) An immunohistochemical mapping of AGBL2 antibody staining in renal cancer tissue as opposed to normal renal tissue, where positive staining is indicated by a brown color (40×). The bar graphs are quantitative analyses of pathology sections from six patients with kidney cancer, and the pictures show images of pathology sections from three cancer patients.

chamber was charged with 500 μl of medium fortified with 20 % fetal bovine serum. Following a 24-h incubation period, the cells inhabiting the lower chamber were collected, fixed with 4 % paraformaldehyde for a span of 15 min, and stained with crystal violet for an additional 15 min.In parallel, the Cell Counting Kit-8 (CCK-8) assay was performed by plating cells at a density ranging from 2 to 3 $\times 10^3$ per well in a 96-well format. After treatment intervals of 24, 48, 72, and 96 h, 10 ml of CCK-8 solution was added to each well, with subsequent incubation extending for 2–4 h. Absorbance readings were captured at a wavelength of 450 nm to provide quantitative insights.Additionally, a colony formation assay was conducted by seeding cells at a density of 1000 per well in a 6-well plate. Following an incubation duration spanning 1–2 weeks, individual colonies were visualized via crystal violet staining, thereby revealing pertinent insights into the clonogenic potential of the cells under examination.

2.8. Data mining

To investigate AGBL2 expression at the transcriptional level in renal cancer, data were extracted from various databases including TIMER 2.0 (http://timer.cistrome.org/), The Cancer Genome Atlas (TCGA) (http://tcga-data.nci.nih.gov/tcga), and Gene Expression Omnibus (GEO) (https://www.ncbi.nlm.nih.gov/gds/). Comprehensive analysis of the clinical attributes and prognostic relevance of AGBL2 in renal cancer patients was facilitated through the utilization of R packages including ggplot [20], pROC [21], survminer [22], and rms [23], drawing upon information from the TCGA database. Furthermore, insights into alterations in the immune microenvironment related to AGBL2 were discerned through the examination of data obtained from the TISIDB database (http://cis.hku.hk/TISIDB/) and again from TIMER 2.0 [24].

2.9. Statistical analyses

Differential expression statistical analysis was performed using the Wilcoxon signed-rank test through GraphPad Prism 8 (GraphPad Software, La Jolla, CA, USA). Data, derived from sequenced datasets such as TCGA and GEO, were systematically analyzed using the R (version 4.2.1) language statistical package (ggplot2 [3.3.6], stats [4.2.1], car [3.1–0]) [25]. Results were depicted as mean ± standard deviation and further evaluated within GraphPad Prism 8. Intergroup comparisons were conducted through either the unpaired two-tailed Student's t-test or Mann-Whitney *U* test, depending on data distribution. The Spearman correlation test was applied to assess relationships between variables, with a p-value <0.05 set as the threshold for statistical significance. The entire approach exemplifies a coherent integration of various statistical tools for mining and analyzing sequencing data. Each experiment was repeated at least 3 times.

3. Results

3.1. AGBL2 is upregulated in renal cell carcinoma

In the present study, we engaged TIMER 2.0 to methodically investigate the expression profile of AGBL2 across a spectrum of cancers as well as in normal tissues (Fig. 1A). Our analysis discerned an elevated expression of AGBL2 in a diverse array of malignancies, including Kidney Renal Clear Cell Carcinoma (KIRC), Kidney Renal Papillary Cell Carcinoma (KIRP), Breast Invasive Carcinoma (BRCA), Esophageal Carcinoma (ESCA), Glioblastoma Multiforme (GBM), Head and Neck Squamous Cell Carcinoma (HNSC), Liver Hepatocellular Carcinoma (LIHC), and Stomach Adenocarcinoma (STAD). Conversely, AGBL2 expression was found to be attenuated in Kidney Chromophobe (KICH), Lung Squamous Cell Carcinoma (LUSC), Pancreatic Adenocarcinoma (PAAD), and Thyroid Carcinoma (THCA). Utilizing the TCGA database, a pronounced overexpression of AGBL2 was discerned in 541 instances of clear cell renal cell carcinoma (KIRC) tissues, in contrast to 72 corresponding pairs of normal tissues (Fig. 1B and C). This observation was corroborated by employing the GEO dataset GSE781, encompassing 6 paired samples (Fig. 1D).

The elevated expression of AGBL2 was corroborated in renal cancer tissues procured from the First Affiliated Hospital of Nanchang University (Fig. 1E), a finding that was further substantiated in associated renal cancer cell lines (Fig. 1F). Immunohistochemical staining analyses were leveraged to determine the protein expression levels of AGBL2 in renal cancer, based on a comparison between six paired samples of renal cancer tissues and their normal counterparts (Fig. 1G). Collectively, these findings converge on a common theme underscoring the significant upregulation of AGBL2 expression in renal cancer, reflecting its potential implication in the oncogenic process.

3.2. Clinical value of AGBL2

As demonstrated in Fig. 2A, both univariate and multivariate Cox regression analyses positioned AGBL2 as an independent risk
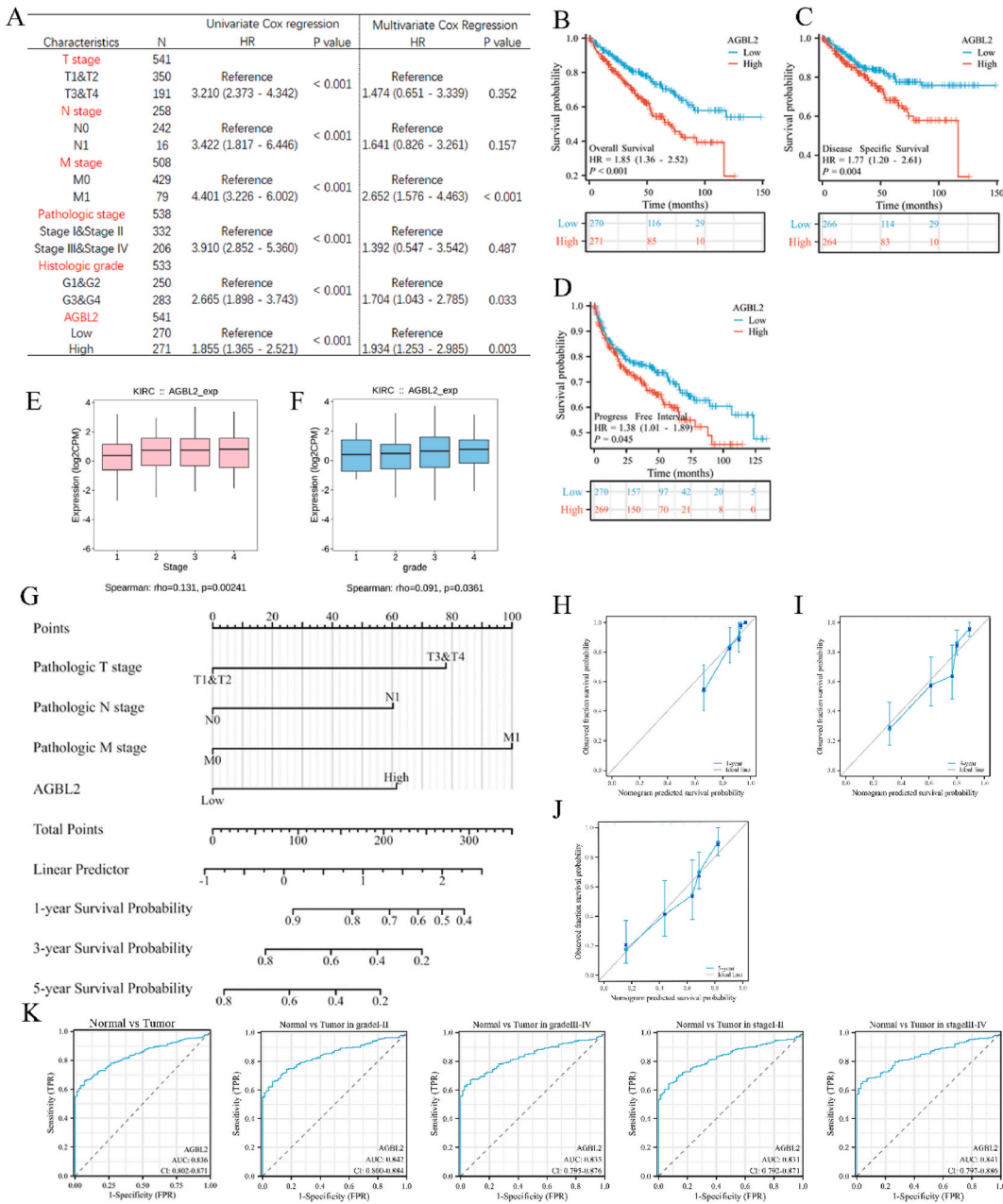
Fig. 2. Clinical value of AGBL2 (A) Implementation of univariate Cox regression analysis and multivariate Cox regression analysis to evaluate the associations in renal cancer. (B–D) Illustration of Kaplan-Meier survival curves displaying the relationships between AGBL2 expression and Overall Survival (OS), Disease-Specific Survival (DSS), and Progression-Free Interval (PFI) in patients with Kidney Renal Clear Cell Carcinoma (KIRC). (E, F) Examination of the pathological stage and histological grade of renal cancer, with reference to AGBL2 expression, drawing on data sourced from TISIDB. (G–J) Construction of a nomogram to represent AGBL2 expression in renal cancer patients, accompanied by performance calibration graphs to assess predictive accuracy. (K) Presentation of Receiver Operating Characteristic (ROC) curves to highlight the diagnostic relevance of AGBL2 expression within the context of renal cancer.

factor for renal cancer, suggesting its role in unfavorable prognosis for kidney renal clear cell carcinoma (KIRC). To discern the relationship between AGBL2 expression and survival outcomes for KIRC patients, Kaplan-Meier survival plots were applied. Fig. 2B–D reveal that patients with higher AGBL2 expression levels endured worse overall survival (OS: HR = 1.85 (1.36–2.52), p < 0.001), disease-specific survival (DSS: HR = 1.77 (1.20–2.61), p = 0.004), and progression-free interval (PFI: HR = 1.38 (1.01–1.89), p = 0.045). TISIDB data additionally correlated AGBL2 expression with advanced pathologic staging (Fig. 2E) and increased histologic grade (Fig. 2F) in kidney cancer patients. Subsequently, we utilized the R packages survminer and rms to construct column-line plots, amalgamating pathologic TNM grading with AGBL2 expression. These plots predicted 1-, 3-, and 5-year survival outcomes for renal
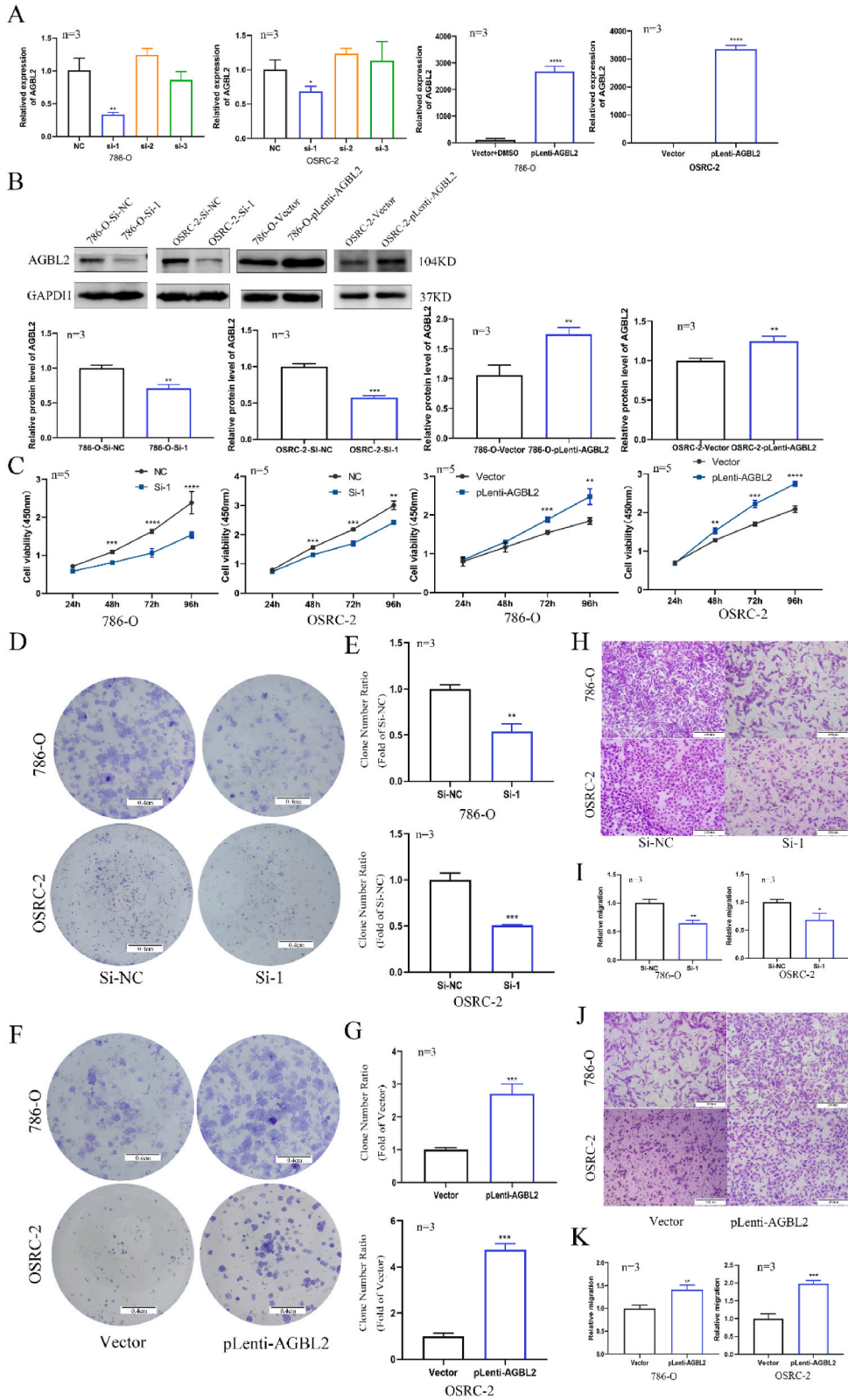
(caption on next page)

Fig. 3. AGBL2 promotes RCC cells migration and proliferation (A, B) Evaluation of the efficiency of AGBL2 knockdown and overexpression in renal cancer cell lines 786-O and OSRC-2; NC denotes negative control. (C–G) Investigation into alterations in cellular proliferation capacity following the knockdown and overexpression of AGBL2, as observed in plate clones and the CCK-8 assay. (H–L) Examination of changes in the migratory abilities of 786-O and OSRC-2 cells in Transwell assays, consequent to either knockdown or overexpression of AGBL2; Scale bars represent 200 μm. Each experiment was repeated at least three times ("n" in the picture indicates the number of experimental data), with statistical significance denoted as $*p < 0.05$; $**p < 0.01$; $***p < 0.001$; $****p < 0.0001$.

cancer patients (Fig. 2G). Impressively, this graphical representation not only exhibited a high predictive precision for overall survival in kidney cancer, with a C-index of 0.764, but also produced calibration plots (Fig. 2H–J) that demonstrated a striking congruence with the predictive model. Finally, we assessed AGBL2's diagnostic value in renal cancer through receiver operating characteristic (ROC) curve analysis. Impressively, AGBL2 manifested robust diagnostic efficacy across various cohorts, achieving an area under the ROC curve greater than 0.83 (Fig. 2K). In conclusion, our findings firmly establish that elevated AGBL2 expression is intricately linked with an adverse prognosis in renal cancer. These insights not only underscore AGBL2's potential as a prognostic marker but also emphasize its promise as an innovative diagnostic tool.

3.3. AGBL2 promotes RCC cells migration and proliferation

To elucidate the role of AGBL2 in renal cancer, we systematically probed its effects in RCC cell lines (786-O and OSRC-2), employing phenotyping experiments. Specifically, AGBL2 expression was modulated through either silencing via siRNA or over-expression via the pLenti-CMV-AGBL2-GFP-Puro vector. Verification of these effects was achieved by leveraging reverse transcription-quantitative PCR (RT-qPCR) and Western blot (WB) analyses (Fig. 3A and B). The Transwell migration assays revealed that AGBL2 inhibition led to a marked decrease in the migration ability of 786-O and OSRC-2 cells (Fig. 3H and I), while its upregulation stimulated the migratory propensity of 786-O and OSRC-2 cells (Fig. 3J and K). Furthermore, the knockdown of AGBL2 led to a discernible reduction in both colony formation and overall cellular growth within renal cancer cell populations (Fig. 3C–E). In stark contrast, the forced upregulation of AGBL2 resulted in a significant enhancement of cell proliferation, as evidenced by the experimental data (Fig. 3C–F,G). These experimental conditions were carefully controlled, utilizing Si-NC or Vector as the reference group, ensuring the reliability of our findings. Collectively, our results illuminate AGBL2's pivotal role in modulating both migration and proliferation of renal cancer cells in vitro, a conclusion that dovetails with the inferences drawn from preceding bioinformatics analyses.

3.4. AGBL2 facilitates renal cancer progression via increased α-tubulin detyrosination

AGBL2, identified as the enzyme catalyzing the detyrosination of α-tubulin, manifests tubulin carboxypeptidase (TCP) activity and functions in the stabilization of microtubules (MTs) [26]. Lopes et al. [9]. reported that detyrosinated α-tubulin accrues near kinetochore-telomeres (KTs) and MT complexes during mitosis, a phenomenon correlated with mitotic aberrations. This suggests that the TCP activity of AGBL2 may play a role through the mechanisms mentioned above. In support of this proposition, our immuno-fluorescence results (Fig. 4A) reveal a predominant nuclear localization of AGBL2. Experimentation confirms that AGBL2 knockdown in RCC cells diminishes detyrosinated α-tubulin, while its overexpression augments the detyrosination levels of α-tubulin (Fig. 4B).

To probe the consequences of AGBL2-mediated detyrosination on the proliferation and migration behaviors of RCC cells, we treated 786-O cells overexpressing AGBL2 with parthenolide, a specialized inhibitor of tubulin carboxypeptidase (TCP). We noted that the detyrosination of α-tubulin, catalyzed by AGBL2, was inhibited by parthenolide in a dose-dependent manner (Fig. 4C). The administration of parthenolide elicited a partial inhibition of the AGBL2-induced increase in both the proliferative (Fig. 4D and E) and migratory capacities (Fig. 4F) of RCC cells. Taken together, these findings underscore AGBL2's role in influencing RCC cell behavior, at least in part, through the modulation of α-tubulin detyrosination.

3.5. AGBL2 impacts multiple biological processes and correlates with immune infiltration

To elucidate the underlying mechanisms of AGBL2 in RCC cells, we extracted total RNA from three AGBL2-silenced 786-O cell groups (Si-1) and three negative controls (Si-NC), and subjected them to transcriptome sequencing analysis. Fig. S1 displays a heat map illustrating the clustering of differentially expressed genes between these groups, revealing that genes up-regulated in the AGBL2 knockdown group (Si-1) were down-regulated in the control group (Si-NC), and vice versa. We performed a comprehensive analysis of the differentially expressed genes between the two groups and utilized a volcano plot to illustrate their distribution, as shown in Supplementary Fig. 2. Compared to the control group, the AGBL2 knockdown group exhibited 170 significantly up-regulated genes and 201 down-regulated genes. Subsequently, We conducted Gene Ontology (GO) and Kyoto Encyclopedia of Genes and Genomes (KEGG) analyses on the differentially expressed genes, with the results depicted in Fig. 5A and B, respectively. The data strongly indicate that the AGBL2 gene has a complex association with various signaling pathways, such as JAK-STAT, MAPK, Toll-like receptor, and p53 signaling pathways. The results derived from Gene Set Enrichment Analysis (GSEA), as detailed in Fig. 5.1C and Supplementary Fig. 3, corroborate this connection. These pathways are known to be intricately linked to cancer development [27–30], emphasizing the potential role of AGBL2 as a vital indicator within tumor-associated signaling pathways.

We also found significant associations with immune signaling pathways, including IL-17, chemokine, and primary immunodeficiency (Fig. 5.1 A, B), as well as with immune-related pathways like Fc epsilon RI signaling and innate immune response in mucosa
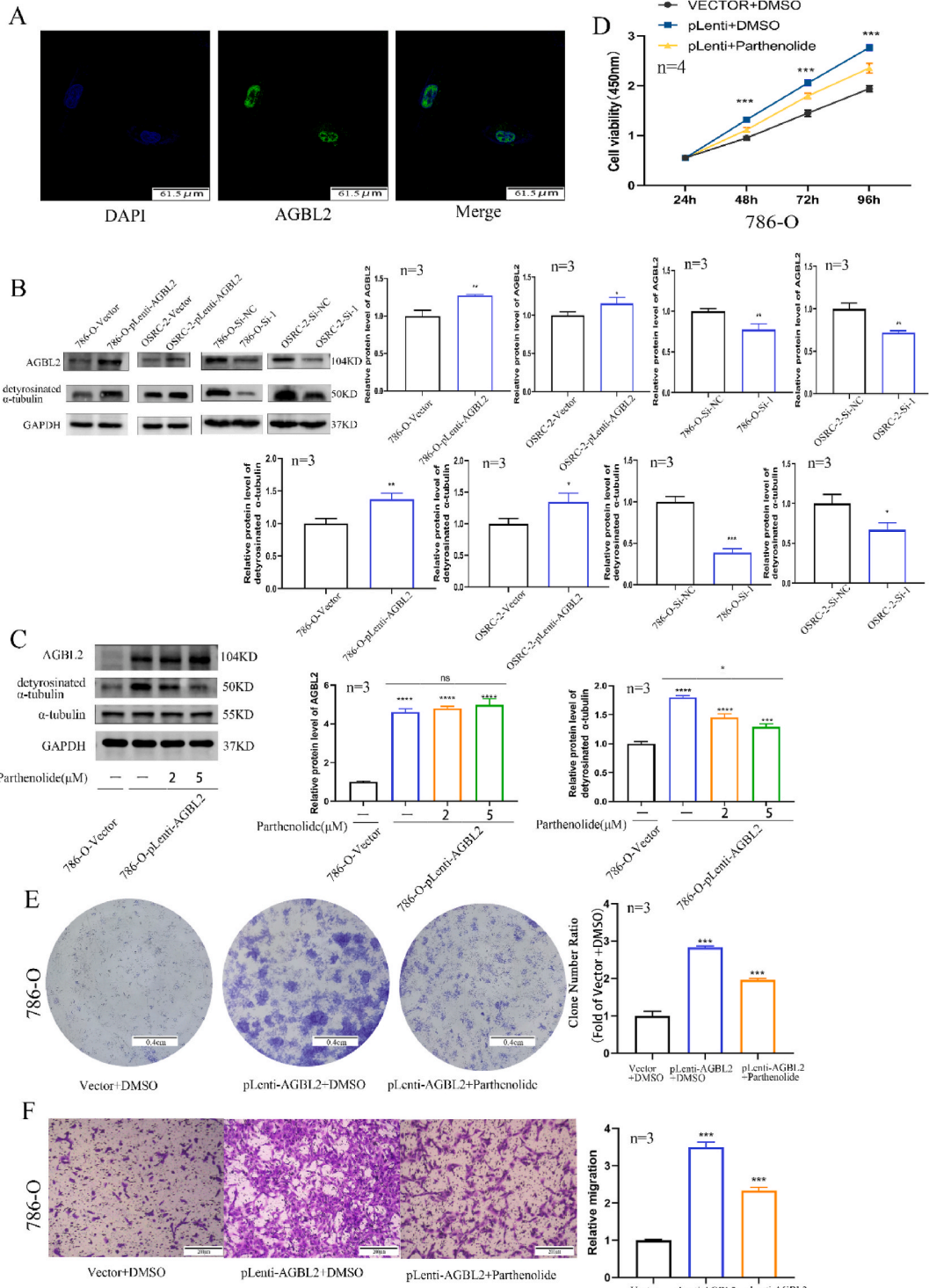
(caption on next page)

Fig. 4. AGBL2 facilitates renal cancer progression via increased α-tubulin detyrosination. (A) Visualization of the intracellular localization of AGBL2 (indicated in green) by immunofluorescence experiments, with nuclear staining depicted in blue. Scale bars represent 61.5 μm (B) Western blot analysis to assess AGBL2 knockdown (Si-1) and overexpression (pLenti-AGBL2), as well as detyrosinated α-tubulin levels in 786-O and OSRC-2 cell lines, utilizing GAPDH as an internal reference. The results of Western Blotting were quantified using histograms. Data (n = 3) were analyzed. (C) Western blot analysis of AGBL2, detyrosinated tubulin, and GAPDH in 786-O cells infected with lentiviral solution (pLenti-CMV-AGBL2-GFP-Puro or vector), and treated with DMSO (negative control) or a designated concentration of parthenolide (0, 2, 5 μmol/L) for 48 h, data (n = 3) were analyzed. (D,E)786-O cells were infected with lentiviral solution (pLenti-CMV-AGBL2-GFP-Puro or vector), incubated for 48 h, and assayed for proliferation in the presence of DMSO (negative control) or 5 μmol/L parthenolide, data (n = 4) were analyzed. (F) 786-O cells, infected with lentiviral solution (pLenti-CMV-AGBL2-GFP-Puro or vector) and incubated for 48 h, were assayed for migratory capacity in the presence of DMSO (negative control) or 5 μmol/L parthenolide. Each experiment was repeated at least three times ("n" in the picture indicates the number of experimental data), with statistical significance denoted as *$p < 0.05$; **$p < 0.01$; ***$p < 0.001$; ****$p < 0.0001$.

(Fig. 5.1 D), through our GSEA analysis. For the analysis of the correlation between AGBL2 and immune infiltration in renal carcinoma (TCGA-KIRC, 539 KIRC tissues), we utilized the R package GSVA [31]. The findings indicated that AGBL2 exhibited a negative correlation with the degree of infiltration of iDC, tgd, and mast cells, while showing a positive correlation with T helper cells (Fig. 5.1 E,F). Additionally, the TISIDB database revealed positive correlations between AGBL2 and two immunosuppressive factors (CD160 and CTLA4), as well as negative correlations with two immune cells (iDC and Monocyte) in renal cancer (Fig.5.2 G). These insights emphasize AGBL2's connection to immunosuppression in renal cancer. Subsequently, we conducted an analysis of the correlation between AGBL2 expression and immune subtypes in renal cancer using the TISIDB database. As shown in the results (Fig. 5.2 H), AGBL2 expression was found to be highest in the INF-γ dominant subtype and lowest in the immunologically quiet subtype. Meanwhile, we investigated the impact of AGBL2 expression and immune cell infiltration on the survival of KIRC patients, date from TIMER2.0. Our observations revealed that decreased levels of Tregs (T-regulatory cells, p = 0.00808), activated NK cells (p = 0.0139), MDSC (Myeloid-derived suppressor cells, p = 0.00186), and T cell follicular helper (p = 0.000451) infiltration were correlated with improved survival in the AGBL2 high expression group (Fig. 5.2 I). These findings imply that renal cancer patients with elevated AGBL2 expression and abundant immune cell subtypes may experience shorter survival times. Taken together, these results suggest that AGBL2 might play a direct or indirect role in immune infiltration in renal cancer, thereby potentially impacting patient prognosis.

3.6. AGBL2 promotes AKT phosphorylation

Our analysis of the above-mentioned sequencing data revealed that AGBL2 is engaged in numerous phosphorylation processes, encompassing phosphatase activity (Fig. 6A–E). Phosphorylation events in various molecules, such as AKT phosphorylation, have been empirically linked to an array of biological functions, including cell proliferation, apoptosis, and signaling [32,33]. Moreover, AKT phosphorylation has been shown to have substantial implications for the development of cancers, including RCC [34,35]. Another enzyme within the TCP family, VASH2, has been recognized for its multifaceted roles across various cancer types, maintaining a close and intricate association with the AKT phosphorylation signaling pathway [36]. This evidence alludes to the potential of AGBL2, as a member of the TCP enzyme family, to modulate the phosphorylation status of AKT in RCC cells. Our experimental results unequivocally demonstrated that AGBL2 overexpression led to a significant increase in AKT phosphorylation in RCC cells, an effect that remained consistent even following treatment with parthenolide (Fig. 6F). Such observations underscore AGBL2's capability to stimulate AKT phosphorylation independent of its detyrosination activity, thereby unraveling another putative mechanism underlying AGBL2's function in renal cancer cells.

4. Discussion

AGBL2 has previously been identified as a significant factor across a range of cancers, encompassing liver, breast, ovarian, gastric, and renal cancer. In hepatocellular carcinoma, Wang et al. [18]. reported that have elucidated that AGBL2 contributes to the growth of cancer cells by regulating IRGM-controlled autophagy and augmenting Aurora A activity. Zhang et al. [14] have marked AGBL2 as an independent prognostic determinant for breast cancer, while similar conclusions were reached by He et al. [37]. for ovarian carcinoma. Zhu et al. [38]. reported that AGBL2 is associated with cell proliferation and chemoresistance in gastric cancer. Importantly, Peterfi et al. [39]. linked the co-expression of RARRES1 and AGBL2 with disease outcomes in RCC, although the detailed expression pattern of AGBL2 in RCC remained unexplored. Within our investigation, we discerned a prominent increase in AGBL2 expression in renal cancer tissues and cell lines, correlating strongly with adverse histologic grade and pathological stage in RCC patients. Kaplan-Meier analysis revealed that high AGBL2 expression was significantly associated with poorer survival outcomes (OS, DSS and PFI) in KIRC. Cox analysis, prognostic nomograms and calibration curves showed that AGBL2 could serve as an important prognostic indicator for KIRC. Moreover, ROC curve analysis revealed high diagnostic utility in AGBL2 expression levels. To further validate the outcomes of our bioinformatics analysis, we utilized siRNA and lentivirus to establish knockdown and overexpression models of AGBL2, aiming to confirm its impact on the proliferation and migration of renal cancer cell lines. AGBL2 knockdown markedly suppressed cell proliferation and migration in RCC cells, whereas its overexpression substantially enhanced migration and cell proliferation in RCC cells.

Microtubules (MTs), essential constituents of the cytoskeleton, are vital in the construction of various subcellular organelles. These architectural proteins regulate fundamental biological processes, including cell growth and motility. Composed of α- and β-microtubulin heterodimers, MTs are dynamic structures undergoing constant morphological shifts throughout the cell cycle, known as
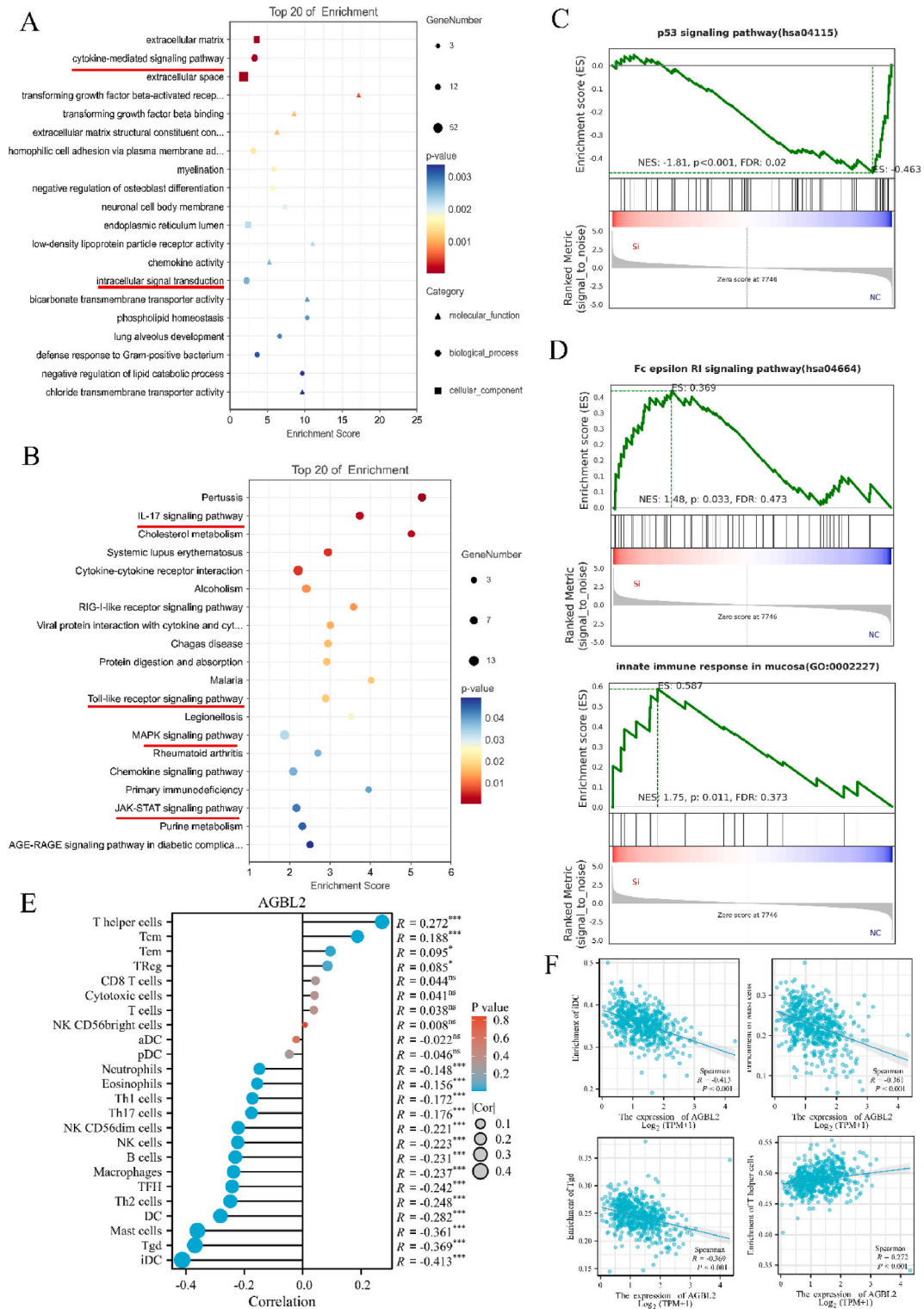
Figure 5a. AGBL2 impacts multiple biological processes and correlates with immune infiltration. (A,B) Plots of GO and KEGG enrichment analyses for genes differing between the two groups. (C,D) Pathway enrichment analysis comparing AGBL2 knockout to control cells; NC denotes negative control.(E) Immune cell infiltration associated with AGBL2 in KIRC, based on TCGA data.(F) Correlation between AGBL2 expression and iDC, Mast cells, Tgd, and T helper cells in renal cancer, based on TCGA data.
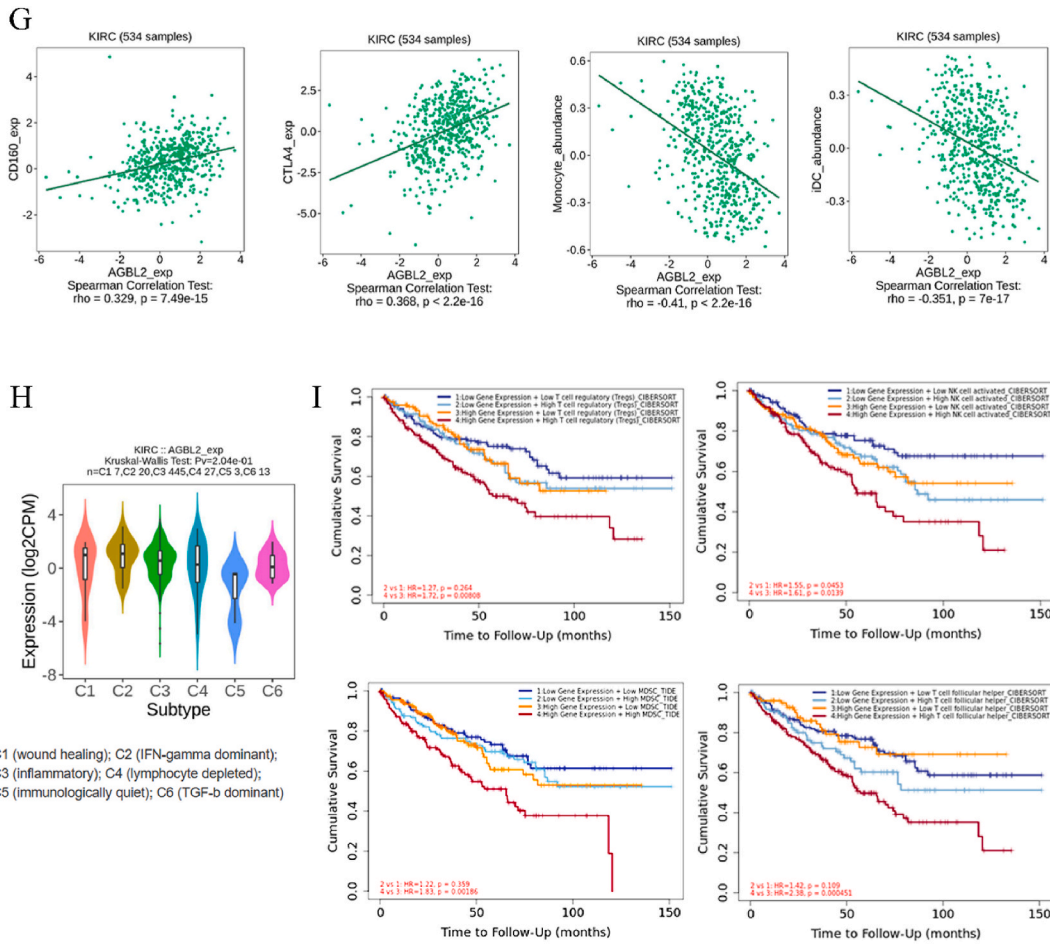
Figure 5b. AGBL2 impacts multiple biological processes and correlates with immune infiltration. (G) Analysis of AGBL2 expression correlation with two immunosuppressive factors (CD160 and CTLA4) and two immune cells (iDC and Monocyte), using TISIDB data.(H) Alterations in AGBL2 expression related to the infiltration of immune subpopulations, date from the TISIDB.(I) Kaplan-Meier profile of AGBL2 gene expression in KIRC, categorized by different levels of immune cell infiltration, date from TIMER2.0.

dynamic instability [3].Numerous studies have provided evidence that post-translational modifications of MTs play a crucial role in various diseases, serving as key regulators of microtubule function. A correlation between the diminished acetylation of microtubule proteins and Parkinson's disease was identified by Godena et al. [40]. In a separate study, Iancu-Rubin et al. [41]. found that aberrant acetylation of microtubule proteins interferes with platelet formation, through the modulation of megakaryocyte maturation. Additionally, Phyo et al. [42]. revealed a process wherein the de-tyrosination of microtubule networks fosters cardiac mast cell growth, ultimately culminating in contractile dysfunction in heart failure patients. These post-translational modifications primarily encompass polyglutamylation, polyglycylation, phosphorylation, acetylation, tyrosination, and detyrosination. Recent studies have indicated that de-tyrosination of the C-terminal Tyr residue of α-tubulin enhances MTs stability. Fluctuations in α-tubulin detyrosination and the responsible enzymes have been observed in various cancers. A study by Wasylyk et al. [43]. revealed that tubulin tyrosine ligase-like 12 (TTLL12) might contribute to prostate cancer progression by reducing the levels of de-tyrosylated microtubule proteins. In another investigation, Kato et al. [44]. elucidated how the expression of hTTL interferes with the regulation of the microtubule protein tyrosine/de-tyrosine cycle, a dysregulation that has been associated with the increase in primary neuroblastoma. Additionally, an observation of elevated levels of de-tyrosinated microtubule proteins in inflammatory breast cancer was reported by Putcha et al. [45]. However, there is a dearth of studies exploring the relationship between AGBL2 and α-tubulin in renal cancer. In our study, we found that AGBL2 knockdown decreased, while its overexpression increased, the detyrosination level of α-tubulin in renal cancer cells. We also discovered that the AGBL2 effect could be partially inhibited by the TCP inhibitor parthenolide, indicating that AGBL2's promotive action may be partly mediated through α-tubulin detyrosination. Surprisingly, we detected high AGBL2 expression in RCC cells' nucleus. Based on the findings of Lopes et al. [14], we theorize that AGBL2-mediated α-tubulin detyrosination could affect kinetochore-telomeres (KTs) and MTs complexes, leading to impaired mitotic error correction and an increased frequency of mitotic errors. These mechanisms might play critical roles in the initiation and progression of renal cancer tumorigenesis. However, comprehensive understanding of renal carcinogenesis's underlying mechanism necessitates further exploration.
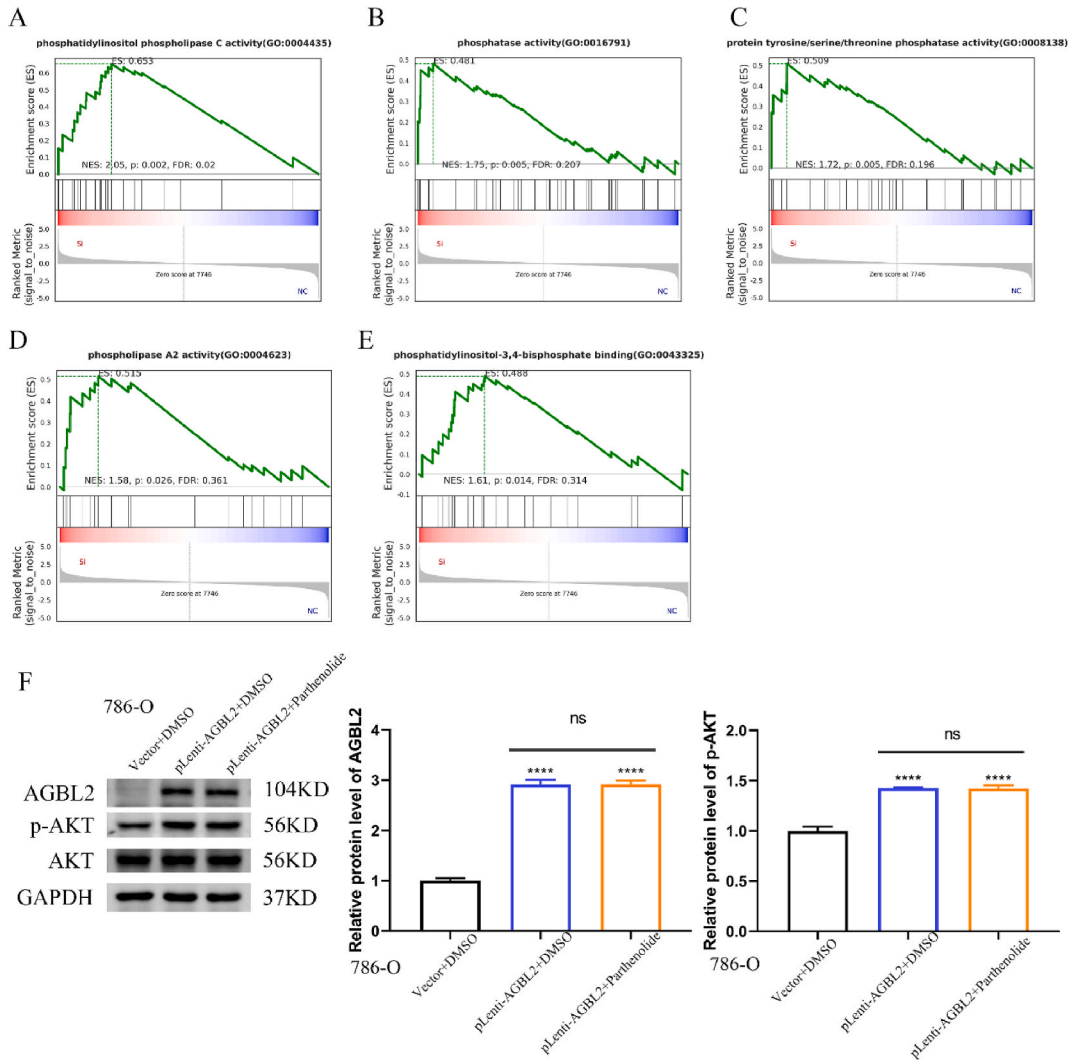
Fig. 6. AGBL2 promotes AKT phosphorylation. (A–E) Pathway enrichment analysis comparing AGBL2 knockout with control cells; NC denotes negative control.(F) Western blot analysis of AGBL2, p-AKT, AKT and GAPDH in 786-O cells infected with lentiviral solution (pLenti-CMV-AGBL2-GFP-Puro or vector) and treated with DMSO (negative control) or 5 μmol/L parthenolide. Data (n = 3)were analyzed, with statistical significance denoted as *p < 0.05; **p < 0.01; ***p < 0.001; ****p < 0.0001.

In an effort to elucidate the molecular mechanism underlying AGBL2's function in KIRC, we embarked on a comprehensive transcriptome sequencing analysis, comparing differentially expressed genes and their affiliated signaling pathways between the AGBL2 knockout and control groups. Through Gene Ontology (GO), Kyoto Encyclopedia of Genes and Genomes (KEGG), and Gene Set Enrichment Analysis (GSEA), we identified connections between AGBL2 and key signaling pathways, including JAK-STAT, MAPK, Toll-like receptor, p53, and VEGF. These findings not only underscore AGBL2's pivotal role in multiple cellular processes but also signify its potential involvement in renal cancer pathogenesis. The data gleaned from this study provide insight into AGBL2's pivotal role within intracellular signaling pathways, shedding light on its potential significance in renal cancer pathogenesis.

Additionally, our further analysis revealed a significant association of AGBL2 with immunotransduction signaling pathways, including the IL-17 signaling pathway and chemokine signaling pathway. RCC, an immunogenic tumor, triggers immune dysfunction primarily via immunosuppressive cell infiltration into the tumor milieu. While checkpoint inhibition is the standard treatment for advanced RCC, a significant subset of patients fails to respond [46]. Consequently, the quest for dependable biomarkers to gauge checkpoint blockade responsiveness is essential to augment the therapeutic efficacy. In this investigation, a robust correlation was discerned between AGBL2 expression and immune cell infiltration in KIRC, including iDC, tgd, and mast cells. These observations provide preliminary evidence of AGBL2's role in immune modulation within the renal cancer milieu. In this study, we have proposed, for the first time, the potential involvement of AGBL2 in the tumor immune microenvironment of renal cancer. Moreover, our findings indicate that the interplay between AGBL2 and immune cells may have implications for the prognosis of renal cancer patients. These insights emphasize the importance of AGBL2 in tumor-immune interactions and beckon further exploration of its potential as a

prognostic marker in renal cancer.

Elevated phosphorylation levels of AKT have been consistently observed across a spectrum of human malignancies, including renal cell carcinoma (RCC), underscoring its pivotal role in oncogenic progression [35,47]. Conclusive research has corroborated that inhibiting AKT phosphorylation not only suppresses renal tumor growth but also enhances chemosensitivity [48,49]. Informed by GSEA analysis, we unearthed a nexus between AGBL2 and various phosphorylation events within renal cell carcinoma. This prompted an in-depth exploration of the interplay between AGBL2 and AKT in RCC cells. The results revealed a significant upregulation of AKT phosphorylation upon AGBL2 overexpression, and interestingly, this effect remained unaltered even after treatment with parthenolide. This indirectly suggests that the reduction in the level of α-tubulin detyrosination does not affect the level of AKT phosphorylation. We also attempted to explore whether knockdown of AGBL2 affects the phosphorylation level of AKT, however, unfortunately, we conducted many studies in which reduced levels of AGBL2 expression did not affect AKT phosphorylation. The reason for this phenomenon may be that the expression level of AGBL2 is inherently low in renal cancer cells. There are almost no studies on the phosphorylation of AKT in relation to the α-tubulin detyrosination, only some articles have reported that the reduction hyperacetylation of a-tubulin can lead to the dephosphorylation of AKT and ultimately lead to cancer cell death [50]. The relationship between phosphorylation of AKT and the α-tubulin detyrosination still needs to be studied further. Collectively, these insights furnish novel evidence that AGBL2 may modulate RCC pathogenesis by upregulating AKT phosphorylation, a mechanism seemingly independent of AGBL2's tubulin carboxypeptidase function.

Although our study provides a comprehensive analysis of AGBL2's mechanism of action in renal cancer, it is imperative to recognize certain inherent limitations. First, additional experimental validation is requisite to thoroughly probe the transduction mechanisms, immune-related functions, and potential interplay with other signaling pathways of AGBL2 in renal cancer. Second, despite demonstrating AGBL2's impact on KIRC cell functionality through in vitro assays, validation through in vivo models remains to be conducted. Third, the precise elucidation of the mechanisms governing AGBL2's regulation of AKT phosphorylation, its implications on tumor progression, and therapeutic responsiveness in renal cancer necessitates further investigations. In conclusion, this work signifies the maiden systematic exploration into AGBL2's role in renal cancer, encompassing extensive analyses employing public databases, high-throughput sequencing techniques, and experimental validations.

5. Conclusion

In conclusion, this study marks the first demonstration, to our knowledge, of a notable association between elevated AGBL2 expression and unfavorable prognosis in KIRC patients. We elucidated the role of AGBL2 in accelerating RCC cell proliferation and metastasis via its influence on the detyrosination level of α-tubulin and observed its capacity to enhance the phosphorylation level of AKT. Further, our data intimate that AGBL2 is entwined with various signaling pathways and immune cell infiltration within renal cancer. These findings collectively advocate AGBL2's substantial potential as a promising diagnostic and therapeutic avenue for the treatment of RCC.

Ethics statements

The investigation involving human participants was conducted in compliance with ethical standards and received approval from the Ethics Committee of the First Affiliated Hospital of Nanchang University (Ethics Committee No. (2022) CDYFYYLK (10–011)). Informed written consent was obtained from all patients or participants involved in this study.

Funding

Data availability statement

Data will be made available on request. Public data are accessible via the provided links in the article, and high-throughput sequencing and experimental data can be obtained from the corresponding author upon reasonable request.

Consent to publish

All authors read and approved the submission of this manuscript.

CRediT authorship contribution statement

Wei Liu: Writing – review & editing, Writing – original draft, Methodology, Investigation, Formal analysis, Data curation, Conceptualization. **Yifei Zhang:** Software. **Yechen Nie:** Writing – original draft, Visualization, Validation, Methodology, Data curation. **Yifu Liu:** Validation, Supervision, Software, Data curation. **Zhongqi Li:** Visualization, Validation. **Zhicheng Zhang:** Formal analysis, Data curation. **Binbin Gong:** Writing – review & editing, Validation, Supervision, Conceptualization. **Ming Ma:** Writing – review & editing, Resources, Project administration, Data curation, Conceptualization.

Declaration of competing interest

The authors declare that they have no known competing financial interests or personal relationships that could have appeared to influence the work reported in this paper.

Appendix A. Supplementary data

Supplementary data to this article can be found online at https://doi.org/10.1016/j.heliyon.2024.e37086.

References

[1] J.J. Hsieh, M.P. Purdue, S. Signoretti, et al., Renal cell carcinoma, Nat Rev Dis Primers 3 (2017) 17009, https://doi.org/10.1038/nrdp.2017.9. Published 2017 Mar 9.
[2] H. Sung, J. Ferlay, R.L. Siegel, et al., Global cancer statistics 2020: GLOBOCAN estimates of incidence and mortality worldwide for 36 cancers in 185 countries, CA Cancer J Clin 71 (3) (2021) 209–249, https://doi.org/10.3322/caac.21660.
[3] R.L. Siegel, K.D. Miller, A. Jemal, Cancer statistics, 2017, CA Cancer J Clin 67 (1) (2017) 7–30, https://doi.org/10.3322/caac.21387.
[4] E. Nogales, Structural insight into microtubule function, Annu. Rev. Biophys. Biomol. Struct. 30 (2001) 397–420, https://doi.org/10.1146/annurev.biophys.30.1.397.
[5] O. Valiron, N. Caudron, D. Job, Microtubule dynamics, Cell. Mol. Life Sci. 58 (14) (2001) 2069–2084, https://doi.org/10.1007/PL00000837.
[6] O. Wattanathamsan, V. Pongrakhananon, Post-translational modifications of tubulin: their role in cancers and the regulation of signaling molecules, Cancer Gene Ther. 30 (4) (2023) 521–528, https://doi.org/10.1038/s41417-021-00396-4.
[7] M.M. Magiera, C. Janke, Post-translational modifications of tubulin, Curr. Biol. 24 (9) (2014) R351–R354, https://doi.org/10.1016/j.cub.2014.03.032.
[8] D.R. Webster, G.G. Gundersen, J.C. Bulinski, G.G. Borisy, Differential turnover of tyrosinated and detyrosinated microtubules, Proc. Natl. Acad. Sci. U.S.A. 84 (24) (1987) 9040–9044, https://doi.org/10.1073/pnas.84.24.9040.
[9] D. Lopes, H. Maiato, The tubulin code in mitosis and cancer, Cells 9 (11) (2020) 2356, https://doi.org/10.3390/cells9112356. Published 2020 Oct 26.
[10] Y. Hu, Q. Xie, X. Wu, et al., Tension of plus-end tracking protein Clip170 confers directionality and aggressiveness during breast cancer migration, Cell Death Dis. 13 (10) (2022) 856, https://doi.org/10.1038/s41419-022-05306-6. Published 2022 Oct 8.
[11] J. Martínez-Hernández, J. Parato, A. Sharma, et al., Crosstalk between acetylation and the tyrosination/detyrosination cycle of α-tubulin in Alzheimer's disease, Front. Cell Dev. Biol. 10 (2022) 926914, https://doi.org/10.3389/fcell.2022.926914. Published 2022 Aug 26.
[12] X. Yu, X. Chen, M. Amrute-Nayak, et al., MARK4 controls ischaemic heart failure through microtubule detyrosination, Nature 594 (7864) (2021) 560–565, https://doi.org/10.1038/s41586-021-03573-5.
[13] K.B. Margulies, B.L. Prosser, Tubulin detyrosination: an emerging therapeutic target in hypertrophic cardiomyopathy, Circ Heart Fail 14 (1) (2021) e008006, https://doi.org/10.1161/CIRCHEARTFAILURE.120.008006.
[14] D. Lopes, A.L. Seabra, B. Orr, H. Maiato, α-Tubulin detyrosination links the suppression of MCAK activity with taxol cytotoxicity, J. Cell Biol. 222 (2) (2023) e202205092, https://doi.org/10.1083/jcb.202205092.
[15] R.A. Whipple, M.A. Matrone, E.H. Cho, et al., Epithelial-to-mesenchymal transition promotes tubulin detyrosination and microtentacles that enhance endothelial engagement, Cancer Res. 70 (20) (2010) 8127–8137, https://doi.org/10.1158/0008-5472.CAN-09-4613.
[16] R. Iida-Norita, M. Kawamura, Y. Suzuki, et al., Vasohibin-2 plays an essential role in metastasis of pancreatic ductal adenocarcinoma, Cancer Sci. 110 (7) (2019) 2296–2308, https://doi.org/10.1111/cas.14041.
[17] Z.J. Sahab, M.D. Hall, Sung Y. Me, et al., Tumor suppressor RARRES1 interacts with cytoplasmic carboxypeptidase AGBL2 to regulate the α-tubulin tyrosination cycle, Cancer Res. 71 (4) (2011) 1219–1228, https://doi.org/10.1158/0008-5472.CAN-10-2294.
[18] L.L. Wang, X.H. Jin, M.Y. Cai, et al., AGBL2 promotes cancer cell growth through IRGM-regulated autophagy and enhanced Aurora A activity in hepatocellular carcinoma, Cancer Lett. 414 (2018) 71–80, https://doi.org/10.1016/j.canlet.2017.11.003.
[19] H. Zhang, Y. Ren, D. Pang, C. Liu, Clinical implications of AGBL2 expression and its inhibitor latexin in breast cancer, World J. Surg. Oncol. 12 (2014) 142, https://doi.org/10.1186/1477-7819-12-142. Published 2014 May 7.
[20] Ginestet CJJotRSS: ggplot2: elegant graphics for data analysis 174 (1) (2011) 245–246.
[21] X. Robin, N. Turck, A. Hainard, et al., pROC: an open-source package for R and S+ to analyze and compare ROC curves, BMC Bioinf. 12 (2011) 77, https://doi.org/10.1186/1471-2105-12-77. Published 2011 Mar 17.
[22] A. Kassambara, Drawing Survival Curves Using 'ggplot2' [R Package Survminer Version 0.2.0], 2017.
[23] F.E. Harrell, F. Harrell, F.E. Harrell, Rms: regression modeling strategies, R package version 4.0-0 (2013).
[24] T. Li, J. Fu, Z. Zeng, et al., TIMER2.0 for analysis of tumor-infiltrating immune cells, Nucleic Acids Res. 48 (W1) (2020) W509–W514, https://doi.org/10.1093/nar/gkaa407.
[25] Y. Liao, G.K. Smyth, W. Shi, The R package Rsubread is easier, faster, cheaper and better for alignment and quantification of RNA sequencing reads, Nucleic Acids Res. 47 (8) (2019) e47, https://doi.org/10.1093/nar/gkz114.
[26] Z.J. Sahab, M.D. Hall, Sung Y. Me, et al., Tumor suppressor RARRES1 interacts with cytoplasmic carboxypeptidase AGBL2 to regulate the α-tubulin tyrosination cycle, Cancer Res. 71 (4) (2011) 1219–1228, https://doi.org/10.1158/0008-5472.CAN-10-2294.
[27] D. Shang, Y. Liu, N. Ito, T. Kamoto, O. Ogawa, Defective Jak-Stat activation in renal cell carcinoma is associated with interferon-alpha resistance, Cancer Sci. 98 (8) (2007) 1259–1264, https://doi.org/10.1111/j.1349-7006.2007.00526.x.
[28] Y. Liu, H. Lv, X. Li, et al., Cyclovirobuxine inhibits the progression of clear cell renal cell carcinoma by suppressing the IGFBP3-AKT/STAT3/MAPK-Snail signalling pathway, Int. J. Biol. Sci. 17 (13) (2021) 3522–3537, https://doi.org/10.7150/ijbs.62114. Published 2021 Aug 13.
[29] H. Ronkainen, P. Hirvikoski, S. Kauppila, et al., Absent Toll-like receptor-9 expression predicts poor prognosis in renal cell carcinoma, J. Exp. Clin. Cancer Res. 30 (1) (2011) 84, https://doi.org/10.1186/1756-9966-30-84. Published 2011 Sep. 19.
[30] A.P. Noon, N. Vlatković, R. Polański, et al., p53 and MDM2 in renal cell carcinoma: biomarkers for disease progression and future therapeutic targets? Cancer 116 (4) (2010) 780–790, https://doi.org/10.1002/cncr.24841.
[31] S. Hänzelmann, R. Castelo, J. Guinney, GSVA: gene set variation analysis for microarray and RNA-seq data, BMC Bioinf. 14 (2013) 7, https://doi.org/10.1186/1471-2105-14-7. Published 2013 Jan 16.
[32] A. Brunet, A. Bonni, M.J. Zigmond, et al., Akt promotes cell survival by phosphorylating and inhibiting a Forkhead transcription factor, Cell 96 (6) (1999) 857–868, https://doi.org/10.1016/s0092-8674(00)80595-4.
[33] Y. Li, J. Xia, N. Jiang, et al., Corin protects H2O2-induced apoptosis through PI3K/AKT and NF-κB pathway in cardiomyocytes, Biomed. Pharmacother. 97 (2018) 594–599, https://doi.org/10.1016/j.biopha.2017.10.090.
[34] C. Porta, C. Paglino, A. Mosca, Targeting PI3K/Akt/mTOR signaling in cancer, Front. Oncol. 4 (2014) 64, https://doi.org/10.3389/fonc.2014.00064. Published 2014 Apr 14.

[35] Q. Zhu, A.L. Zhong, H. Hu, et al., Acylglycerol kinase promotes tumour growth and metastasis via activating the PI3K/AKT/GSK3β signalling pathway in renal cell carcinoma, J. Hematol. Oncol. 13 (1) (2020) 2, https://doi.org/10.1186/s13045-019-0840-4. Published 2020 Jan 3.

[36] X. Tan, Z. Liao, S. Zou, L. Ma, A. Wang, VASH2 promotes cell proliferation and resistance to doxorubicin in non-small cell Lung cancer via AKT signaling, Oncol. Res. 28 (1) (2020) 3–11, https://doi.org/10.3727/096504019X15509383469698.

[37] W.P. He, L.L. Wang, High expression of AGBL2 is a novel prognostic factor of adverse outcome in patients with ovarian carcinoma, Oncol. Lett. 18 (5) (2019) 4900–4906, https://doi.org/10.3892/ol.2019.10829.

[38] H. Zhu, Z. Zheng, J. Zhang, et al., Effects of AGBL2 on cell proliferation and chemotherapy resistance of gastric cancer, Hepato-Gastroenterology 62 (138) (2015) 497–502.

[39] L. Peterfi, D. Banyai, M.V. Yusenko, T. Bjercke, G. Kovacs, Expression of RARRES1 and AGBL2 and progression of conventional renal cell carcinoma, Br. J. Cancer 122 (12) (2020) 1818–1824, https://doi.org/10.1038/s41416-020-0798-6.

[40] V.K. Godena, N. Brookes-Hocking, A. Moller, et al., Increasing microtubule acetylation rescues axonal transport and locomotor deficits caused by LRRK2 Roc-COR domain mutations, Nat. Commun. 5 (2014) 5245, https://doi.org/10.1038/ncomms6245. Published 2014 Oct 15.

[41] C. Iancu-Rubin, D. Gajzer, G. Mosoyan, F. Feller, J. Mascarenhas, R. Hoffman, Panobinostat (LBH589)-induced acetylation of tubulin impairs megakaryocyte maturation and platelet formation, Exp. Hematol. 40 (7) (2012) 564–574, https://doi.org/10.1016/j.exphem.2012.02.004.

[42] S.A. Phyo, K. Uchida, C.Y. Chen, et al., Transcriptional, post-transcriptional, and post-translational mechanisms rewrite the tubulin code during cardiac hypertrophy and failure, Front. Cell Dev. Biol. 10 (2022) 837486, https://doi.org/10.3389/fcell.2022.837486. Published 2022 Apr 1.

[43] C. Wasylyk, A. Zambrano, C. Zhao, et al., Tubulin tyrosine ligase like 12 links to prostate cancer through tubulin posttranslational modification and chromosome ploidy, Int. J. Cancer 127 (11) (2010) 2542–2553, https://doi.org/10.1002/ijc.25261.

[44] C. Kato, K. Miyazaki, A. Nakagawa, et al., Low expression of human tubulin tyrosine ligase and suppressed tubulin tyrosination/detyrosination cycle are associated with impaired neuronal differentiation in neuroblastomas with poor prognosis, Int. J. Cancer 112 (3) (2004) 365–375, https://doi.org/10.1002/ijc.20431.

[45] P. Putcha, J. Yu, R. Rodriguez-Barrueco, et al., HDAC6 activity is a non-oncogene addiction hub for inflammatory breast cancers [published correction appears in Breast Cancer Res. 2017 Apr 19;19(1):49], Breast Cancer Res. 17 (1) (2015) 149, https://doi.org/10.1186/s13058-015-0658-0. Published 2015 Dec 8.

[46] C.M. Díaz-Montero, B.I. Rini, J.H. Finke, The immunology of renal cell carcinoma, Nat. Rev. Nephrol. 16 (12) (2020) 721–735, https://doi.org/10.1038/s41581-020-0316-3.

[47] Y. He, M.M. Sun, G.G. Zhang, et al., Targeting PI3K/Akt signal transduction for cancer therapy, Signal Transduct Target Ther 6 (1) (2021) 425, https://doi.org/10.1038/s41392-021-00828-5. Published 2021 Dec 16.

[48] P.J. Vlachostergios, A.M. Molina, PI3K/AKT inhibitors in patients with refractory renal cell carcinoma: what have we learnt so far? Ann. Oncol. 28 (5) (2017) 914–916, https://doi.org/10.1093/annonc/mdx104.

[49] S. Hara, M. Oya, R. Mizuno, A. Horiguchi, K. Marumo, M. Murai, Akt activation in renal cell carcinoma: contribution of a decreased PTEN expression and the induction of apoptosis by an Akt inhibitor, Ann. Oncol. 16 (6) (2005) 928–933, https://doi.org/10.1093/annonc/mdi182.

[50] Q.Y. Zhu, Z. Wang, C. Ji, et al., C6-ceramide synergistically potentiates the anti-tumor effects of histone deacetylase inhibitors via AKT dephosphorylation and α-tubulin hyperacetylation both in vitro and in vivo, Cell Death Dis. 2 (1) (2011) e117, https://doi.org/10.1038/cddis.2010.96. Published 2011 Jan 27.